

SUPPORTING INFORMATION

FOR

Chemiluminescent Biosensors for Detection of Second Messenger Cyclic di-GMP

Andrew B. Dippel¹, Wyatt A. Anderson¹, Robert S. Evans², Samuel Deutsch^{2,3,4}, and Ming C. Hammond^{1,5}*

¹Department of Chemistry, University of California, Berkeley, 94720, USA

²DOE Joint Genome Institute, 2800 Mitchell Drive, Walnut Creek, CA 94598, USA

³Environmental Genomics and Systems Biology Division, and ⁴Biological Systems and Engineering Division, Lawrence Berkeley National Laboratory, 1 Cyclotron Road, Berkeley, CA 94720, USA

⁵Department of Molecular & Cell Biology, University of California, Berkeley, 94720, USA

*Corresponding author

Table of Contents

Additional methods	S3-S5
Figure S1. Workflow for lysate-based biosensor assay.....	S6
Figure S2. Lysate-based screen of <i>EcYcgR</i> biosensor mutant and linker variants.....	S7
Figure S3. Analysis of mCherry tag as measure of biosensor stability.....	S8
Figure S4. Lysate-based screen of phylogenetic library variants.....	S9
Figure S5. In vitro characterization of biosensor variants.....	S10
Table S1. Oligonucleotides used in this study.....	S11-S12
Table S2. Phylogenetic sequence variants.....	S13-S16
Table S3. Amino acid sequences of biosensor plasmids.....	S17
Table S4. Nucleotide sequences of biosensor plasmids.....	S18-S19
Supplemental Notes	S20-S21
References	S21

ADDITIONAL METHODS

General reagents and oligonucleotides. Cyclic dinucleotides were purchased from Axxora, LLC. Coelenterazine-h was purchased from NanoLight Technologies and stored as a ~6.15 mM stock in EtOH at -80 °C. Oligonucleotides used in molecular cloning were purchased from Elim Biopharmaceuticals.

Molecular cloning. The pRSET_B-Nano-lantern plasmid was a gift from Takeharu Nagai (Addgene plasmid # 51969). Plasmids encoding YhjH, WspR alleles, and PleD were available in our lab. For expression and purification, all biosensor constructs were cloned into the pRSET_B plasmid between the NdeI and EcoRI sites with an N-terminal His-tag. Overlap-extension PCR was used to add the three N-terminal residues back to RLuc8 to create pRSET_B-Nano-lantern (1.1). All NL biosensor constructs using *EcYcgR* were cloned into pRSET_B using Gibson Assembly¹ in which both linear backbone and insert fragments were amplified by PCR. The *EcYcgR* sequence was amplified from BL21 Star genomic DNA and mutant alleles were generated using site-directed mutagenesis. For lysate or live-cell based experiments, YNL and *EcYcgR* biosensor constructs were amplified by PCR and ligated into pET21 and/or pET24 plasmids between NdeI and HindIII sites and included a C-terminal His-tag. To create mCherry tagged versions of these plasmids, mCherry was amplified by PCR to add a flexible linker (GSGGSGGS) at the N-terminus then ligated between BamHI and HindIII sites of the empty plasmid to generate pET21-linker-mCherry and pET24-linker-mCherry. YNL and *EcYcgR* biosensor constructs were then amplified by PCR and ligated into the pET21- or pET24-linker-mCherry plasmid between NdeI and BamHI sites.

Protein purification. *E. coli* BL21 (DE3) Star cells (Life Technologies) were transformed with the pRSET_B vector encoding N-terminally His-tagged NL biosensor variants. Transformants were cultured in 2xYT medium at 37 °C until OD reached ~0.8–1.0, followed by induction of protein expression with 0.1 mM IPTG for 20 h at 20 °C. Cells were collected and lysed by sonication in lysis buffer [50 mM Tris (pH 7.5), 150 mM NaCl, 20 mM imidazole, 5% (v/v) glycerol] with 300 µg/mL lysozyme and 1 mM PMSF added. Clarified lysate was bound to Ni-NTA agarose (Thermo Scientific), and resin was washed with lysis buffer supplemented with 500 mM NaCl prior to elution with lysis buffer supplemented with 300 mM imidazole. Using Amicon Ultra-15 Centrifugal Filter Units (molecular weight cutoff 10 kDa; Millipore), the elution fractions were

concentrated and dialyzed to storage buffer [50 mM HEPES (pH 7.2), 100 mM KCl, 10% (v/v) glycerol]. Concentrated protein was flash frozen in liquid nitrogen then stored at -80 °C in small aliquots to prevent repetitive freeze-thaw cycles. Protein concentrations were determined using the absorption of Venus at 515 nm (extinction coefficient = 92200 M⁻¹ cm⁻¹). In stated cases, cells were co-transformed with the pCOLA-PdeH plasmid lacking a His-tag to enable purification of the biosensor without c-di-GMP bound.

Phylogenetic library generation. YcgR sequence variants employed were selected using the Pfam database. Briefly, Pfam was searched for all PilZ-domain containing proteins with a domain architecture similar to EcYcgR (YcgR-PilZ), which were presumed to undergo conformational changes upon binding c-di-GMP. The query resulted in 840 total sequences (258 sequences with YcgR-PilZ, 582 sequences with YcgR_2-PilZ), then a subset of 92 sequences were chosen for synthesis and cloning into the biosensor scaffold (pET21- and pET24-biosensor-mCherry). All sequences from suspected thermophilic organisms were given priority, and all remaining sequences were chosen from a large variety of bacterial genomes. The selected genes were codon optimized and ‘polished’ to remove DNA synthesis constraints using BOOST.² Double stranded DNA was obtained from Gen9 (Gingko Bioworks). For cloning into the pET21 and pET24 derived vectors using Gibson cloning,¹ 25 bp linkers at the beginning and end of the sequences were included. Eight colonies per construct were sequenced verified using PACBIO RSII system (Pacific Biosciences), and variant calling was performed using the GATK software package.³

Cellular c-di-GMP measurements with biosensor co-expression. Single colonies of BL21(DE3) star *E. coli* cells co-transformed with pET21-biosensor-mCherry plasmids and pCOLA-PdeH or pCOLA-WspR-D70E were resuspended in 500 µL of P-0.5G non-inducing media [0.5% glucose, 25 mM (NH₄)₂SO₄, 50 mM KH₂PO₄, 50 mM Na₂HPO₄, 1 mM MgSO₄]⁴ supplemented with 100 µg/mL kanamycin and 50 µg/mL carbenicillin in 2.2 mL 96-well deep well plates (VWR), then grown at 37 °C, 325 rpm, for 24 h to generate pre-cultures. A 5 µL aliquot of each pre-culture was used to inoculate 500 µL of ZYP-5052 auto-induction media [25 mM (NH₄)₂SO₄, 50 mM KH₂PO₄, 50 mM Na₂HPO₄, 1 mM MgSO₄, 0.5% (v/v) glycerol, 0.05% glucose, 0.2% α-lactose, 1% tryptone, and 0.5% yeast extract]⁴ supplemented with 100 µg/mL kanamycin and 50 µg/mL carbenicillin in a deep well plate and grown at 37 °C, 325 rpm, for 20 h

to allow for protein expression. For live cell measurements, cultures were harvested by centrifugation, media was removed, and cell pellets were resuspended in 500 μ L PBS. A 100 μ L aliquot of each culture was transferred to an opaque white 96-well plate, and the plate was incubated at 28 °C for 10 min. The mCherry fluorescence intensity was measured for each well, 20 μ L chemiluminescent substrate was added manually to each well, and then total chemiluminescence was monitored over 10 min. Luminescent signal was calculated as the total chemiluminescence at 10 min divided by the mCherry fluorescence intensity to normalize differences in biosensor expression between biological replicates.

For lysate measurements, cultures were harvested and clarified lysates were prepared as described for the lysate-based assay for biosensor activity, except each culture was resuspended in 240 μ L screening buffer. A 100 μ L aliquot of each clarified lysate was carefully pipetted into an opaque white 96-well plate, and the plate was incubated at 28 °C for 10 min. The mCherry fluorescence intensity was measured for each well, then chemiluminescent substrate was injected and chemiluminescence was measured as described in the lysate-based assay. Luminescent signal was calculated as the total chemiluminescence divided by the mCherry fluorescence intensity to normalize differences in biosensor expression between biological replicates.

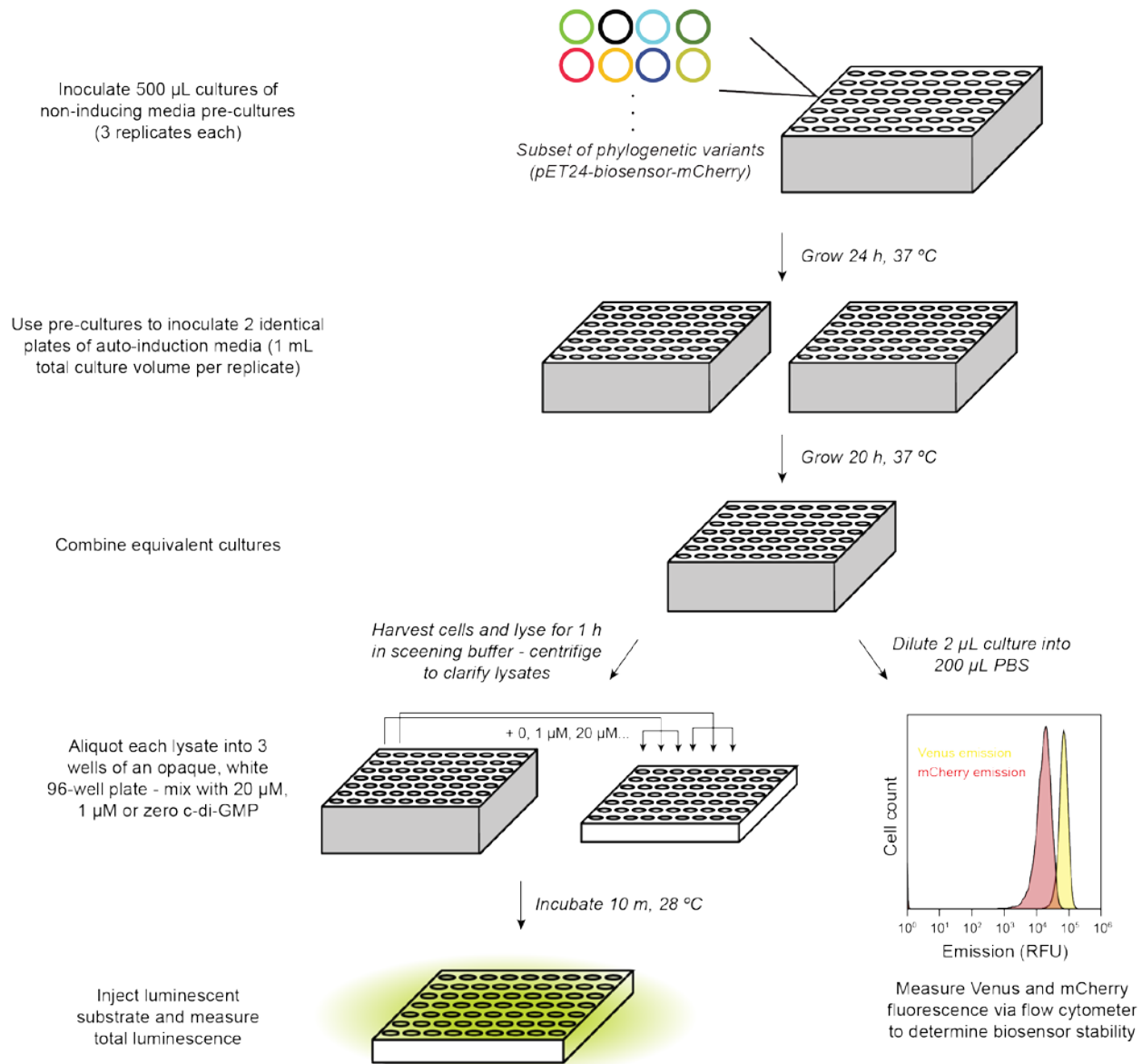


Figure S1. Workflow for lysate-based biosensor assay. *E. coli* transformed with biosensor variants are grown in non-inducing media in deep-well plates to generate pre-cultures. The following day, pre-cultures are used to inoculate auto-induction media and cultures are grown overnight. The next day, a small aliquot of cells is analyzed via flow cytometry to determine relative biosensor expression and stability. The remaining cells are harvested and lysed in screening buffer. Clarified lysates are mixed with c-di-GMP in an opaque white, 96-well plate, chemiluminescent substrate is added, and total chemiluminescent signal is measured to determine signal fold-changes.

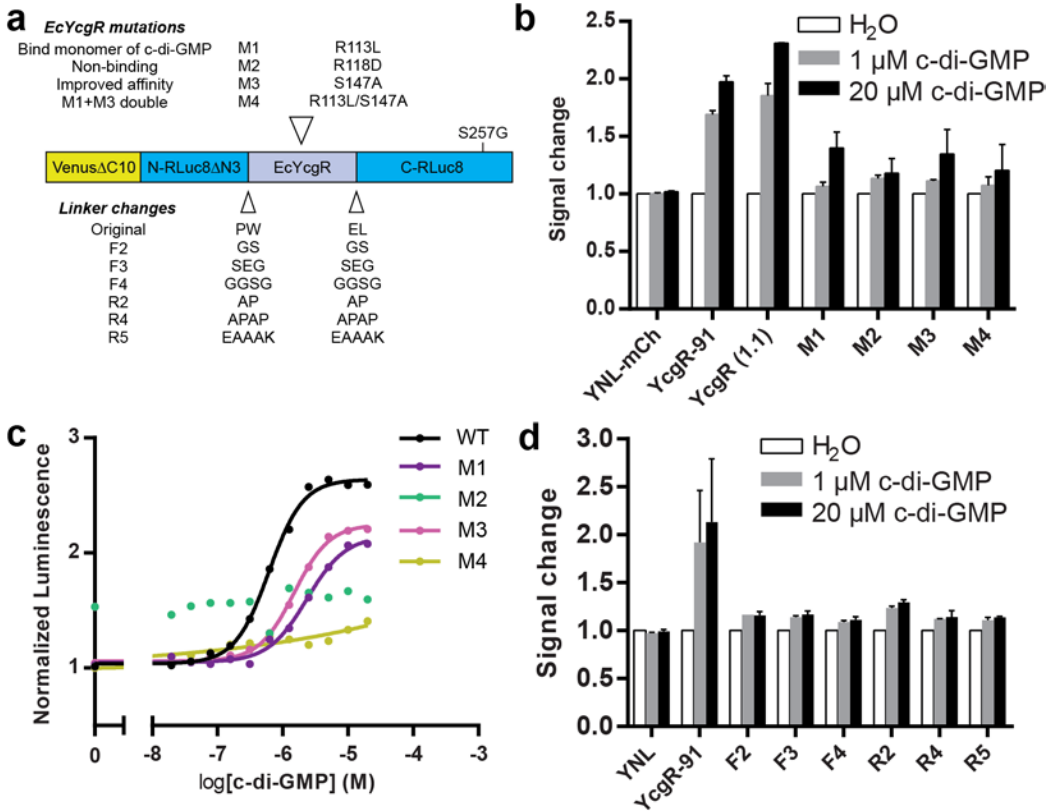


Figure S2. Lysate-based screen of *EcYcgR* biosensor mutant and linker variants. (a) Schematic of *EcYcgR-91* biosensor showing different mutations to *EcYcgR* and the different linkers tested. (b) Signal change for *EcYcgR-91* biosensors and mutants in the lysate-based assay. Data are from 2 biological replicates represented as mean \pm SD. (c) Biosensor binding affinity measurements with purified *EcYcgR-91* mutants. Data are presented as mean of 3 replicates. Error bars are omitted for clarity. (d) Signal change for *EcYcgR-91* linker variants in the lysate-based assay. Data are from 2 biological replicates represented as mean \pm SD.

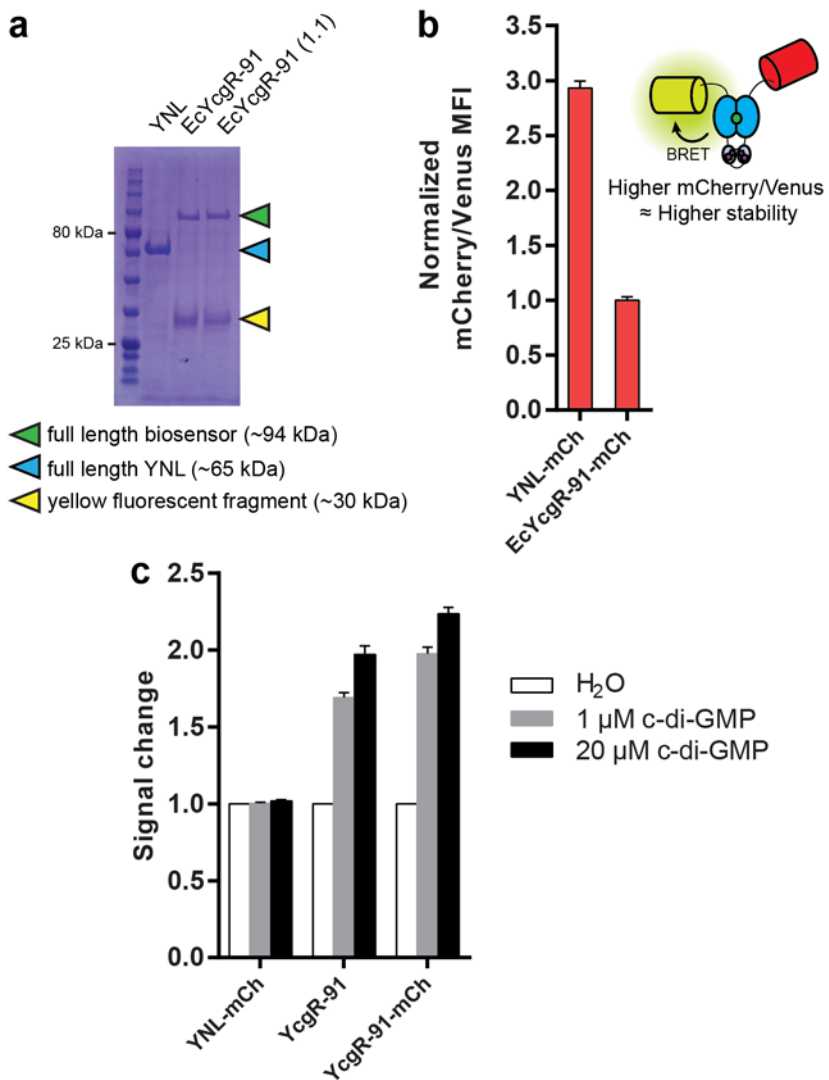


Figure S3. Analysis of mCherry tag as measure of biosensor stability. (a) SDS-PAGE of purified proteins showing presence of truncated protein products for NL biosensor constructs. (b) Normalized mCherry/Venus MFI ratios of cells expressing mCherry tagged NL constructs as measured by flow cytometry. Ratios are normalized to the ratio for EcYcgR-91-mCh and show that the ratio correlates with relative protein stability. Data are from 3 biological replicates represented as mean \pm SD. (c) Signal change for NL constructs in the lysate-based assay show the mCherry tag has no negative effect on biosensor performance. Data are from 2 biological replicates represented as mean \pm SD.

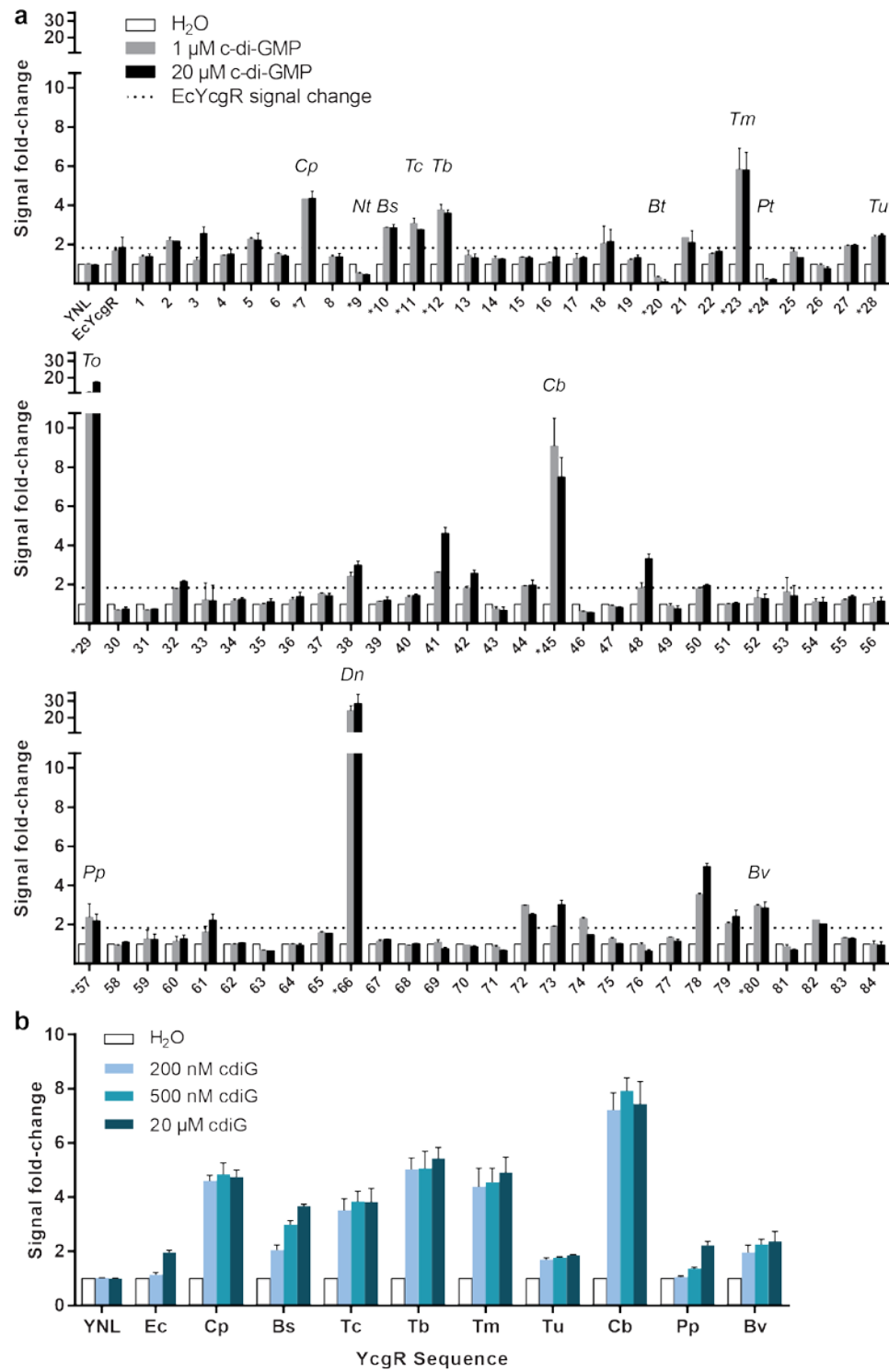


Figure S4. Lysate-based screen of phylogenetic library variants. (a) Signal fold-change for the 84 active phylogenetic biosensor variants. Labeled sequences were chosen for further characterization due to apparent high affinity, large signal change, or negative signal change. See Table S2 for numbering. Data are from 2 biological replicates represented as mean \pm SD. (b) Signal fold-change for selected high affinity variants. Selected variants were re-screened in the lysate-based assay with lower concentrations of c-di-GMP. Data are from 3 biological replicates represented as mean \pm SD.

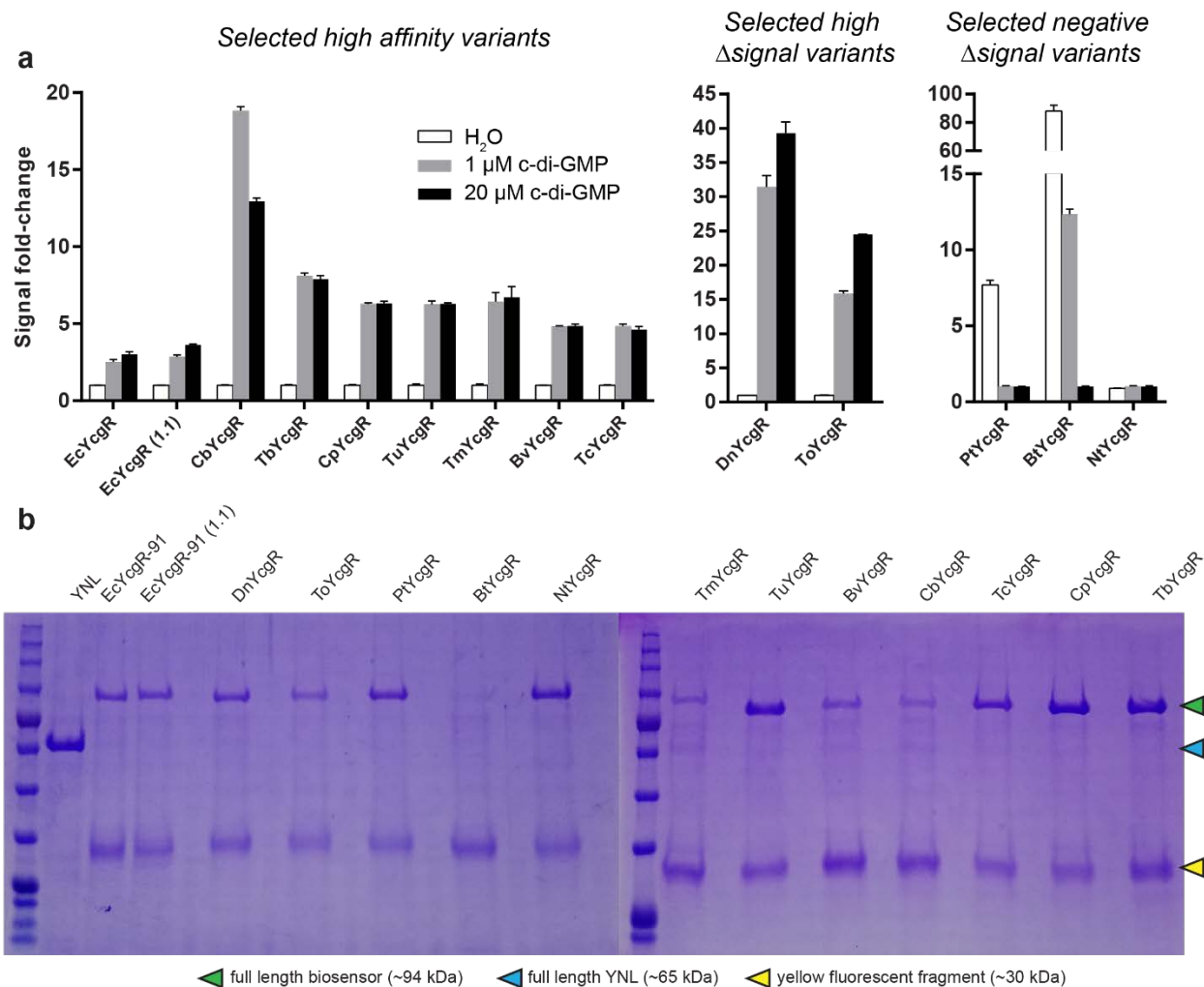


Figure S5. In vitro characterization of biosensor variants. (a) Same data as in Figure 3b, but presented as signal fold-change. Values are normalized to no c-di-GMP for selected high affinity and high Δ signal variants, and values are normalized to 20 μ M c-di-GMP for negative Δ signal variants. Signal change data is summarized in Table 1. Data are from 3 replicates represented as mean \pm SD. (b) SDS-PAGE of all purified biosensor variants used for in vitro characterization showing the presence of a truncated protein product that is fluorescent.

Table S1. Oligonucleotides used in this study

REV-YcgR-R118D-rth	gaaatatcgccgtcggttacaaacc
FWD-YcgR-S147A-rth	Gcgtaggcggcatggg
REV-YcgR-S147A-rth	caaatacatacaggcggaaacg
FWD-YNL-Ndel	tattcacatATGGTGAGCAAGGGCGAGG
REV-YNL-HindIII (no stop)	cgttaagcttCTGCTCGTTCTTCAGCACTCTCTC
REV-YNL-BamHI (no stop)	ataggatccCTGCTCGTTCTTCAGCACTCTCTC
FWD-mCherry w/ linker-BamHI	ataggatccggcggcagcggcggcagcATGGTGAGCAAGGGCGA
REV-mCherry-HindIII (no stop)	tataagcttCTTGTACAGCTCGTCCATGCC
FWD-YNL-pRSET insert	GACGATGACGATAAGgatccgATGGTGAGCAAGGGCGAG
REV-YNL-pRSET insert	CCGGATCAAGCTTCGAATTcTTACTGCTCGTTCTTCAGCACTCTC

Table S2. Phylogenetic sequence variants

Notes: Orange highlighted organism names are predicted thermophiles. Any sequence without a number label (numbering used in Figure S4) produced very low luminescence activity in the lysate-based screen and was not included in any data shown.

UniProt accession	Description	Organism	Domain arch	Length	Number	Name
YCGRL_VIBCH	Cyclic di-GMP binding protein VCA0042	Vibrio cholerae serotype O1 (strain ATCC 39315 / El Tor Inaba N16961)	YcgR2-PilZ	252	1	
YCGR_PSEPK	Flagellar brake protein YcgR	Pseudomonas putida (strain KT2440)	YcgR-PilZ	247	2	
YCGR_SALTY	Flagellar brake protein YcgR	Salmonella typhimurium (strain LT2 / SGSC1412 / ATCC 700720)	YcgR-PilZ	244	3	
Q9HYP3_PSEAE	Uncharacterized protein	Pseudomonas aeruginosa (strain ATCC 15692 / DSM 22644 / CIP 104116 / JCM 14847 / LMG 12228 / 1C / PRS 101 / PAO1)	YcgR-PilZ	263	4	
Q67PC2_SYMTH	Putative uncharacterized protein	Symbiobacterium thermophilum (strain T / IAM 14863)	YcgR2-PilZ	234	5	
R7RRU9_9CLOT	Flagellar protein	Thermobrachium celere DSM 8682	YcgR2-PilZ	223	6	
B5Y7A9_COPPD	Type IV pilus assembly protein PilZ	Coprothermobacter proteolyticus (strain ATCC 35245 / DSM 5265 / BT)	YcgR2-PilZ	233	7	Cp
G0GFW8_SPITZ	Type IV pilus assembly PilZ	Spirochaeta thermophila (strain ATCC 700085 / DSM 6578 / Z-1203)	YcgR2-PilZ	369		
M1E4L7_9FIRM	Type IV pilus assembly PilZ	Thermodesulfobium narugense DSM 14796	YcgR2-PilZ	246	8	
G0GFW8_SPITZ	Type IV pilus assembly PilZ	Spirochaeta thermophila (strain ATCC 700085 / DSM 6578 / Z-1203)	YcgR2-PilZ	357		
B7GHM9_ANOFW	Predicted glycosyltransferase	Anoxybacillus flavithermus (strain DSM 21510 / WK1)	YcgR2-PilZ	239		
B2A369_NATTJ	Type IV pilus assembly PilZ	Natrananerobius thermophilus (strain ATCC BAA-1301 / DSM 18059 / JW/NM-WN-LF)	YcgR2-PilZ	225	9	Nt
A0A150LBE3_9BACI	Uncharacterized protein	Bacillus sporothermodurans	YcgR2-PilZ	216	10	Bs
A1HN17_9FIRM	Type IV pilus assembly PilZ	Thermosinus carboxydivorans Nor1	YcgR2-PilZ	211	11	Tc
A0A124FJ12_9FIRM	Type IV pilus assembly PilZ	Thermoanaerobacterales bacterium 50_218	YcgR2-PilZ	220	12	Tb
D5XFF1_THEPJ	Type IV pilus assembly PilZ	Thermincola potens (strain JR)	YcgR2-PilZ	219	13	
A0A0S3QVC2_9AQUI	Type IV pilus assembly PilZ	Thermosulfidibacter takaii ABI70S6	YcgR2-PilZ	242	14	
B8CYP6_HALOH	Type IV pilus assembly PilZ	Halothermothrix orenii (strain H 168 / OCM 544 / DSM 9562)	YcgR2-PilZ	216	15	
D7CM20_SYNLT	Type IV pilus assembly PilZ	Syntrophothermus lipocalidus (strain DSM 12680 / TGB-C1)	YcgR2-PilZ	216	16	
B0K9S5_THEP3	Type IV pilus assembly PilZ	Thermoanaerobacter pseudethanolicus (strain ATCC 33223 / 39E)	YcgR2-PilZ	209	17	

I3VWB4_THESW	Type IV pilus assembly PilZ	Thermoanaerobacterium saccharolyticum (strain DSM 8691 / JW/SL-YS485)	YcgR2-PilZ	209	18	
K8EBV6_9FIRM	Type IV pilus assembly PilZ	Desulfotomaculum hydrothermale Lam5 = DSM 18033	YcgR2-PilZ	227	19	
A0A090IV04_9BACI	Glycosyltransferase	Bacillus thermoamylovorans	YcgR2-PilZ	220	20	Bt
A8F4V2_PSELT	Type IV pilus assembly PilZ	Pseudothermotoga lettingae (strain ATCC BAA-301 / DSM 14385 / NBRC 107922 / TMO)	YcgR2-PilZ	234	21	
F7YXY9_9THEM	Type IV pilus assembly PilZ	Pseudothermotoga thermarum DSM 5069	YcgR2-PilZ	227	22	
Q9X007_THEMEA	Flagellar protein	Thermotoga maritima (strain ATCC 43589 / MSB8 / DSM 3109 / JCM 10099)	YcgR2-PilZ	229	23	Tm
A5D0H5_PELTS	Glycosyltransferase	Pelotomaculum thermopropionicum (strain DSM 13744 / JCM 10971 / SI)	YcgR2-PilZ	219	24	Pt
D9S3A4_THEOJ	Type IV pilus assembly PilZ	Thermosediminibacter oceanii (strain ATCC BAA-1034 / DSM 16646 / JW/IW-1228P)	YcgR2-PilZ	212	25	
K4LH04_THEPS	Type IV pilus assembly PilZ	Thermacetogenium phaeum (strain ATCC BAA-254 / DSM 12270 / PB)	YcgR2-PilZ	220	26	
A6LMY0_THEME4	Type IV pilus assembly PilZ	Thermosiphlo melanesiensis (strain DSM 12029 / CIP 104789 / BI429)	YcgR2-PilZ	220	27	
A0A101EVB1_9THEM	Type IV pilus assembly PilZ	Thermotoga sp. 50_1627	YcgR2-PilZ	227	28	Tu
LOEE96_THECK	Putative glycosyltransferase	Thermobacillus composti (strain DSM 18247 / JCM 13945 / KWC4)	YcgR2-PilZ	217	29	To
A3DCP7_CLOTH	Type IV pilus assembly PilZ	Clostridium thermocellum (strain ATCC 27405 / DSM 1237 / NBRC 103400 / NCIMB 10682 / NRRL B-4536 / VPI 7372)	YcgR2-PilZ	224	30	
E6SJP9_THEME7	Type IV pilus assembly PilZ	Thermaerobacter marianensis (strain ATCC 700841 / DSM 12885 / JCM 10246 / 7p75a)	YcgR2-PilZ	220	31	
Q2RKC8_MOOTA	Glycosyltransferase-like protein	Moorella thermoacetica (strain ATCC 39073 / JCM 9320)	YcgR2-PilZ	219	32	
D1B6A2_THEAS	Type IV pilus assembly PilZ	Thermanaerovibrio acidaminovorans (strain ATCC 49978 / DSM 6589 / Su883)	YcgR2-PilZ	227	33	
K8EH43_9FIRM	Type IV pilus assembly PilZ	Desulfotomaculum hydrothermale Lam5 = DSM 18033	YcgR2-PilZ	208	34	
H2INW0_RAHAC	Flagellar brake protein YcgR	Rahnella aquatilis (strain ATCC 33071 / DSM 4594 / JCM 1683 / NBRC 105701 / NCIMB 13365 / CIP 78.65)	YcgR-PilZ	248	35	
A0A080M6H4_9PROT	Flagellar brake protein YcgR	Candidatus Accumulibacter sp. SK-02	YcgR-PilZ	266	36	
A0A0R0ARV1_9GAMM	Flagellar brake protein YcgR	Stenotrophomonas panacihumi	YcgR-PilZ	265	37	
A0A063BEK1_9BURK	Flagellar brake protein YcgR	Burkholderia sp. lig30	YcgR-PilZ	251	38	

Q7CK58_YERPE	Flagellar brake protein YcgR	<i>Yersinia pestis</i>	YcgR-PilZ	252	39	
H8GFW9_METAL	Flagellar brake protein YcgR	<i>Methylomicrobium album</i> BG8	YcgR-PilZ	239	40	
B4E8L7_BURCJ	Flagellar brake protein YcgR	<i>Burkholderia cenocepacia</i> (strain ATCC BAA-245 / DSM 16553 / LMG 16656 / NCTC 13227 / J2315 / CF5610)	YcgR-PilZ	251	41	
S6B8T9_9PROT	Flagellar brake protein YcgR	<i>Sulfuricella denitrificans</i> skB26	YcgR-PilZ	257	42	
A0A0D5V569_9BURK	Flagellar brake protein YcgR	<i>Paraburkholderia fungorum</i>	YcgR-PilZ	263	43	
YCGR_LARHH	Flagellar brake protein YcgR	<i>Laribacter hongkongensis</i> (strain HLHK9)	YcgR-PilZ	271	44	
H1SBM0_9BURK	Flagellar brake protein YcgR	<i>Cupriavidus basilensis</i> OR16	YcgR-PilZ	233	45	Cb
E1TCJ5_BURSG	Flagellar brake protein YcgR	<i>Burkholderia</i> sp. (strain CCGE1003)	YcgR-PilZ	263	46	
D8IT03_HERSS	Flagellar brake protein YcgR	<i>Herbaspirillum seropedicae</i> (strain SmR1)	YcgR-PilZ	251	47	
C5AEG4_BURGB	Flagellar brake protein YcgR	<i>Burkholderia glumae</i> (strain BGR1)	YcgR-PilZ	250	48	
YCGR_NITEC	Flagellar brake protein YcgR	<i>Nitrosomonas eutropha</i> (strain C91)	YcgR-PilZ	269		
YCGR_THIDA	Flagellar brake protein YcgR	<i>Thiobacillus denitrificans</i> (strain ATCC 25259)	YcgR-PilZ	255	49	
A0A126T293_9GAMM	Flagellar brake protein YcgR	<i>Methylomonas denitrificans</i>	YcgR-PilZ	249	50	
H5V7W3_ESCHE	Flagellar brake protein YcgR	<i>Escherichia hermannii</i> NBRC 105704	YcgR-PilZ	243	51	
YCGR1_DECAR	Flagellar brake protein YcgR 1	<i>Dechloromonas aromatica</i> (strain RCB)	YcgR-PilZ	264	52	
A9MP65_SALAR	Flagellar brake protein YcgR	<i>Salmonella arizonaee</i> (strain ATCC BAA-731 / CDC346-86 / RSK2980)	YcgR-PilZ	244	53	
E6WB98_PANSA	Flagellar brake protein YcgR	<i>Pantoea</i> sp. (strain At-9b)	YcgR-PilZ	244	54	
S6ALU3_PSERE	Flagellar brake protein	<i>Pseudomonas resinovorans</i> NBRC 106553	YcgR-PilZ	264	55	
YCGR_METML	Flagellar brake protein YcgR	<i>Methylotenera mobilis</i> (strain JLW8 / ATCC BAA-1282 / DSM 17540)	YcgR-PilZ	253	56	
L1LXK9_PSEPU	Uncharacterized protein	<i>Pseudomonas putida</i> CSV86	YcgR-PilZ	247	57	Pp
A0A080MAN3_9PROT	Flagellar brake protein YcgR	<i>Candidatus Accumulibacter</i> sp. BA-91	YcgR-PilZ	259	58	
A0A0L0GIP1_9ENTR	Flagellar brake protein YcgR	<i>Trabulsiella odontotermitis</i>	YcgR-PilZ	243	59	
A0A0K1K509_9BURK	Flagellar brake protein YcgR	<i>Massilia</i> sp. NR 4-1	YcgR-PilZ	253	60	
A0A024HEU5_PSEKB	Flagellar brake protein YcgR	<i>Pseudomonas knackmussii</i> (strain DSM 6978 / LMG 23759 / B13)	YcgR-PilZ	249	61	
A0A0S8DMJ3_9GAMM	Flagellar brake protein YcgR	<i>Gammaproteobacteria</i> bacterium SG8_47	YcgR-PilZ	252	62	

Q97H69_CLOAB	Uncharacterized protein, YPFA B.subtilis ortholog	Clostridium acetobutylicum (strain ATCC 824 / DSM 792 / JCM 1419 / LMG 5710 / VKM B-1787)	YcgR2-PilZ	222	63	
A0A0U9HJ89_9THEO	C-di-GMP-binding flagellar brake protein YcgR	Tepidanaerobacter syntrophicus	YcgR2-PilZ	213	64	
A0A140LAQ7_9THEO	Flagellar brake protein YcgR	Fervidicola ferrireducens	YcgR2-PilZ	212	65	
D4H107_DENA2	Type IV pilus assembly PilZ	Denitrovibrio acetiphilus (strain DSM 12809 / N2460)	YcgR2-PilZ	219	66	Dn
D3PCV1_DEFDS	Type IV pilus assembly protein PilZ	Defribacter desulfuricans (strain DSM 14783 / JCM 11476 / NBRC 101012 / SSM1)	YcgR2-PilZ	223	67	
A8FEM7_BACP2	Pilus assembly protein PilZ	Bacillus pumilus (strain SAFR-032)	YcgR2-PilZ	215	68	
W6N5K7_CLOTY	Flagellar protein	Clostridium tyrobutyricum DIVETGP	YcgR2-PilZ	216	69	
A4J746_DESRM	Type IV pilus assembly PilZ	Desulfotomaculum reducens (strain MI-1)	YcgR2-PilZ	221	70	
A0A151B6Q5_9CLOT	Flagellar protein YcgR	Clostridium tepidiprofundii DSM 19306	YcgR2-PilZ	217	71	
C6C102_DESAD	Type IV pilus assembly PilZ	Desulfovibrio salexigens (strain ATCC 14822 / DSM 2638 / NCIB 8403 / VKM B-1763)	YcgR2-PilZ	229		
A6M180_CLOB8	Type IV pilus assembly PilZ	Clostridium beijerinckii (strain ATCC 51743 / NCIMB 8052)	YcgR2-PilZ	213		
R1AST9_9CLOT	Flagellar protein	Caldsalinibacter kiritimatiensis	YcgR2-PilZ	222	72	
F7NL64_9FIRM	Type IV pilus assembly PilZ	Acetonema longum DSM 6540	YcgR2-PilZ	215	73	
L0FC86_DESDL	Putative glycosyltransferase	Desulfitobacterium dichloroeliminans (strain LMG P-21439 / DCA1)	YcgR2-PilZ	214	74	
R7C6C4_9CLOT	Type IV pilus assembly PilZ	Clostridium sp. CAG:62	YcgR2-PilZ	236	75	
A0A139D977_9FIRM	Flagellar protein	Halanaerobium sp. T82-1	YcgR2-PilZ	213	76	
R7R388_9FIRM	Flagellar protein	Roseburia sp. CAG:100	YcgR2-PilZ	255	77	
A0A0E3W3A0_9FIRM	PilZ domain	Syntrophomonas zehnderi OL-4	YcgR2-PilZ	216	78	
D5CSE9_SIDLE	Type IV pilus assembly PilZ	Sideroxydans lithotrophicus (strain ES-1)	YcgR2-PilZ	311		
I8RFB4_9FIRM	Type IV pilus assembly PilZ	Pelosinus fermentans B4	YcgR2-PilZ	215	79	
Q24T82_DESHY	Putative uncharacterized protein	Desulfitobacterium hafniense (strain Y51)	YcgR2-PilZ	200		
W1SJT3_9BACI	Type iv pilus assembly pilz	Bacillus vireti LMG 21834	YcgR2-PilZ	207	80	Bv
A3WPA0_9GAMM	Predicted glycosyltransferase	Idiomarina baltica OS145	YcgR2-PilZ	233	81	
K8DYS2_9FIRM	Putative Type IV pilus assembly PilZ	Desulfotomaculum hydrothermale Lam5 = DSM 18033	YcgR2-PilZ	209	82	
W0JLH8_DESAE	Uncharacterized protein	Desulfurella acetivorans A63	YcgR2-PilZ	224	83	
A0A0E4HD84_9BACL	Type IV pilus assembly protein PilZ	Paenibacillus riograndensis SBR5	YcgR2-PilZ	186	84	

Table S3: Amino acid sequences of biosensor plasmids

Notes: His-tag, Venus ΔC10, RLuc8 (4-91), EcYcgR, RLuc8 (92-311), mCherry tag;
phylogenetic biosensor variants use the same sequences, except the phylogenetic variant is used
in place of EcYcgR.

PRSET-YNL-EcYcgR-91	MRGSHHHHHGGMASMTGGQQMGRDLYDDDDKDE MVSKEELFTGVVPILVELGDVNGHKFSVSGEGEGD ATYGKLTKLIC CTTGKLPVPWPTLVTTGYGLQCFARYPDHM KQHDFFKSAMPEGYVQERTIFFKDDGNY KTRAEVKFEGDTLVNRIELKGIDFKEDGNILGHKLEYNNNSHNVITADKQKNGIKANFKIRHNIEDGGV QLADHYQQNTPI GDGPVLLPDNH YQS SKLSKDPNEKRDHMV LEFVTAAGGT KVYDPEQRKRM ITGPQ WWARCKQMNVLD LDSFINYYDSEKHAENAVI FLHG NATSSYLWRHVPHIEPVARCIIPD LIGMGKSGKSGN GSPWMSHYHEQFLKQNPLAVLGVLRLHKAAPLRLS SWNGQ LI SKLLA ITPD KLVLD FGSQAE DNI IAVL KAQHITITAETQGA KVEFTVEQLQQSEYLQLPA FTVPPPTLWFVQR RRYFRISAPLHPPYFC QTKLADN STLRFR LYDLSLGGM GALLETAKPAELQEGMRFAQIE EVNMGQWGVFHFD AQ LIS ISERK VIDGKNET ITT PRLSFRFLNV SPTVERQLQRIIFSLEREAREKA D KVRD EYRLLDH KYLTAWFELLNL PKKI IFVGH DW GAALAFHYAYEH QDR IKAI VHME S VV D VIES WD RKLEPEEFAAYLEPFKE GEVRRPTLSWPRE I PLVKGGKPDVVQIVRN YNAYLRAS DDL PKLF IEGDPGF SNA IVEGAKKF P NTEFV KV KGLH FL QEDAP DE MGKYIKSF V ERVL K NEQ KLA AALEHHHHHH *stop
pET21/24-YNL-EcYcgR-91	MVSKEELFTGVVPILVELGDVNGHKFSVSGEGEGDATY GKLT KLIC TTGKLPVPWPTLVTTGYGLQ CFARYPDHM KQHDFFKSAMPEGYVQERTIFFKDDGNY KTRAEVKFEGDTLVNRIELKGIDFKEDGNILGH KLEYNNNSHNVITADKQKNGIKANFKIRHNIEDGGV QLADHYQQNTPIGDGPVLLPDNH YQS SKLSKDPNEKRDHMV LEFVTAAGGT KVYDPEQRKRM ITGPQWWARCKQMNVLD LDSFINYYDSEKHAENAVI FLHG NATSSYLWRHVPHIEPVARCIIPD LIGMGKSGKSGN SPWMSHYHEQFLKQNPLAVLGVLRLHKAAPLRL SWNGQ LI SKLLA ITPD KLVLD FGSQAE DNI IAVLKAQHITITAETQGA KVEFTVEQLQQSEYLQLPA FTVPPPTLWFVQR RRYFRISAPLHPPYFC QTKLADNSTLRFR LYDLSLGGM GALLETAKPAELQEGMRFAQIE EVNMGQWGVFHFD AQ LIS ISERK VIDGKNET ITT PRLSFRFLNV SPTVERQLQRIIFSLEREAREKA D KVRD EYRLLDH KYLTAWFELLNL PKKI IFVGH DWGAALAFHYAYEH QDR IKAI VHME S VV D VIES WD EWPDIEEDIALIKSEE GEKMVL LENFFVETV LPSK IMRKLEPEEFAAYLEPFKE GEVRRPTLSWPRE I LVKGGKPDVVQIVRN YNAYLRAS DDL PKLF IEGDPGF FSNA IVEGAKKF P NTEFV KV KGLH FL QEDAP DE MGKYIKSF V ERVL K NEQ KLA AALEHHHHHH *stop
pET21/24-YNL-EcYcgR-91-mCherry	MVSKEELFTGVVPILVELGDVNGHKFSVSGEGEGDATY GKLT KLIC TTGKLPVPWPTLVTTGYGLQ CFARYPDHM KQHDFFKSAMPEGYVQERTIFFKDDGNY KTRAEVKFEGDTLVNRIELKGIDFKEDGNILGH KLEYNNNSHNVITADKQKNGIKANFKIRHNIEDGGV QLADHYQQNTPIGDGPVLLPDNH YQS SKLSKDPNEKRDHMV LEFVTAAGGT KVYDPEQRKRM ITGPQWWARCKQMNVLD LDSFINYYDSEKHAENAVI FLHG NATSSYLWRHVPHIEPVARCIIPD LIGMGKSGKSGN SPWMSHYHEQFLKQNPLAVLGVLRLHKAAPLRL SWNGQ LI SKLLA ITPD KLVLD FGSQAE DNI IAVLKAQHITITAETQGA KVEFTVEQLQQSEYLQLPA FTVPPPTLWFVQR RRYFRISAPLHPPYFC QTKLADNSTLRFR LYDLSLGGM GALLETAKPAELQEGMRFAQIE EVNMGQWGVFHFD AQ LIS ISERK VIDGKNET ITT PRLSFRFLNV SPTVERQLQRIIFSLEREAREKA D KVRD EYRLLDH KYLTAWFELLNL PKKI IFVGH DWGAALAFHYAYEH QDR IKAI VHME S VV D VIES WD EWPDIEEDIALIKSEE GEKMVL LENFFVETV LPSK IMRKLEPEEFAAYLEPFKE GEVRRPTLSWPRE I LVKGGKPDVVQIVRN YNAYLRAS DDL PKLF IEGDPGF FSNA IVEGAKKF P NTEFV KV KGLH FL QEDAP DE MGKYIKSF V ERVL K NEQ GGGGGS MVS KGEEDNM AI IKEFMRFKVHMEGSVNGHEFIE EE GEGRPYEGTQ TAKLK VTKGGPLP FA DWLSPQFM Y GSKAYV K HPADIP Y LKL S PEGFKWERVMNF EDGGVV TVDQSS L QDGFEIY K VVKL R GTNF PSD GPV M QKKTMGWEASSER M PEDGALK E IKQRL L KLDG G GHYDAEV K TTYK AKKP VQLP G AYNV N IKLDIT SHN EDYTIVE Q YERAEGRH ST GGM DELY K KLA AALEHHHHHH *stop

Table S4: Nucleotide sequences of biosensor plasmids

Notes: Corresponding nucleotide sequences of amino acid sequences presented in Table S3

	tacagcggattatccctcgagcgagaagccggaaaaagcggacaaagtgcgcgacgagctcTAC AGGCTGCTGGACCCTACAAGTACACTGACCCTGAGCTCCTGAACCTGCCAAGAACATCATTT CGTGGGCCACGACTGGGGCGCCgcCCTGGCTTCACTACgcCTACGAGCACCAGGACAgGATCAAGGCCA TCGTGCACatgGAGAGCGTGGTGGACGTGATCGAGAGCTGGGACGAGTGGGCCAGACATCGAGGAGGACATC GCCCTGATCAAGAGCGAGGGAGGGCGAGAAAGATGGTGTGGAGAAACAACCTTCTCGTGGAGACCGTGCTGCC CAGCAAGATCATGAGAAAAGCTGGAGGCCGAGGAGTTCGCCCCCTGGTGAAGGGCGCAAGGCCGACGTGGTG AGGTGAGAAGACCCCACCTGAGCTGGCCAGAGAGATCCCCCTGGTGAAGGGCGCAAGGCCGACGTGGTG CAGATCGTGGAGAAACTACAAGCCTACCTGAGAGCCAGCAGCACCTGCCAAGcTGTTCATCGAGGgcGA CCCCGGCTTCTCAGCAACGCCATCGTGGAGGGCGCCAAGAAGATTCCCCAACACCGAGTTGTGAAGGTGA AGGGCTGCACCCtCCAGGAGGACCCCCCGACAGAGTGGCAAGTACATCAAGAGCTTGTGGAGAGA GTGCTGAAGAACGAGCAGgatccgc GGCCATCATCAAGGAGTTCATCGCCTTAAGGTGCACATGGAGGGCTCCGTGAACGGCCACGAGTTCGAGA TCGAGGGCGAGGGCGAGGGCGCCCCTACGAGGGCACCCAGACCGCCAAGCTGAAGGTGACCAAGGGTGGC CCCCGGCCCTTCGCTGGGACATCTGTCCCCCTCAGTTCATGTACGGCTCAAGGCCACGTGAAGCACC CGCCGACATCCCCGACTACTTGAAGCTGTCCTTCCCCGAGGGCTTCAAGTGGAGCGCGTGTGAACTTCG AGGACGGCGCGTGGTGACCGTAGCCAGGACTCTCCCTGCAGGACGGGAGTTCATCTACAAGGTGAAG CTGCGCGGCCACCAACTTCCCCCTCGACGGGCCGCTGAAGGGCGAGATCAAGCAGAGGCTGAAGCTGAAGGACGGCG GCCACTACGACGCTGAGGTCAAGACCACCTACAAGGCCAAGAAGGCCGACGTGCCCCGCGCTACAAC GTCAACATCAAGTTGGACATCACCTCCACAACGAGGACTACACCATCGTGAACAGTACGAACGCCGA GGGCCGCACTCCACCGGGCATGGACGAGCTGTACAAGAagcttcgcgcgcactcgagcaccaccacc accaccactga
pET21/24- YNL- EcYcgR-91- mCherry	ATGGTGAGCAAGGGCGAGGAGCTGTTCACGGGGTGGTGGCCCATCCTGGTCAGCTGGACGGCAGCTAAA CGGCCACAAGTTCAGCGTGTCCGGCGAGGGCGAGGGCGATGCCACCTACGGCAAGCTGACCCCTGAAGCTGA TCTGCACCACGGCAAGCTGCCGTGCCCTGGCCCACCCCTGTGACCACCTGGCTACGGCCTGCAGTGC TTCGCCCGCTACCCCGACCACATGAAGCAGCACGACTCTTCAAGTCCGCACTGCCAAGGCTACGTCCA GGAGCGCACCATCTTCTCAAGGACGACGGCAACTACAAGACCCGCGAGGTGAAGTTGAGGGCGACA CCCTGGTGAACCGCATCGAGCTGAAGGGCATCGACTCAAGGAGGACGGCAACATCTGGGGCACAAGCTG GAGTACAACATACAACGCCAACGCTATATCACCGCCACAAGCAGAAGAACGGCATCAAGGCCACCT CAAGATCCGCCACAACATCGAGGACGGCGCGTGCAGCTGCCGACCACTACCGCAGAACACCCCCATCG GCGACGGCCCCGTGCTGCTGCCGACAACCAACTACCTGAGCTACCGTCAAGCTGAGCAAAGACCCCAAC GAGAAGCGCGATCACATGGCTCTGCTGGAGTTGTGACCGCCGGGgtaccAAGGTGTACGACCCGA GCAGAGGAAGAGGATGATCACCGGCCCCAGTGGTGGGCCAGGTGCAAGCAGATGAACGTGCTGGACAGCT TCATCAACTACTACGACAGCGAGAACGACGCCGAGAACGCCGTGATCTTCTGCACGGCAACGCCaCTAGC AGCTACCTGTGGAGGCACGTGGTGGCCACATCGAGCCCCTGGCCAGGTGCATCATCCCCGATCTGATCGG CATGGGCAAGAGCGGCAAGAGCGGCAACGGCAGCcattggATGagtcatattaccatgagcagttcctgaaac aaaatccgttagccgtctggcgctgttacgcgatttgacaaagccgcaattccatttcgtctcaatttgg aatggcgcccgactgtatcggcaataaccccgataaaacttgtgatccggatttcggcactgtca agccgaagacaacatccgtctggcgatccggccatccggccatccggccatccggccatccggccatccggcc tcgatccggccatccggccatccggccatccggccatccggccatccggccatccggccatccggccatccggcc cccacccatccggccatccggccatccggccatccggccatccggccatccggccatccggccatccggccatccggcc ccagaccaactggcgataacactgttacgttccggccatccggccatccggccatccggccatccggccatccggcc cattactggaaacagccatccggccatccggccatccggccatccggccatccggccatccggccatccggccatccggcc ggccatgggttttacttgcacccagttacgttccggccatccggccatccggccatccggccatccggccatccggcc gaatggaaaccatcaccactcccgctgagcttccggccatccggccatccggccatccggccatccggccatccggcc tacgcgatccggccatccggccatccggccatccggccatccggccatccggccatccggccatccggccatccggcc AGGTGCTGGACCCTACAAGTACACTGACCCTGAGCTCCTGAACCTGCCAAGAACATCATTT CGTGGGCCACGACTGGGGCGCCgcCCTGGCTTCACTACgcCTACGAGCACCAGGACAgGATCAAGGCCA TCGTGCACatgGAGAGCGTGGTGGACGTGATCGAGAGCTGGGACGAGTGGGACATCGAGGAGGACATC GCCCTGATCAAGAGCGAGGGAGGGCGAGAAAGATGGTGTGGAGAAACAACCTTCTCGTGGAGACCGTGCTGCC CAGCAAGATCATGAGAAAAGCTGGAGGCCGAGGAGTTCGCCCCCTACCTGGAGCCCTTCAAGGAGAACGGCG AGGTGAGAAGACCCCACCTGAGCTGGCCAGAGAGATCCCCCTGGTGAAGGGCGCAAGGCCGACGTGGTG CAGATCGTGGAGAAACTACAAGCCTACCTGAGAGCCAGCAGCACCTGCCAAGcTGTTCATCGAGGgcGA CCCCGGCTTCTCAGCAACGCCATCGTGGAGGGCGCCAAGAAGATTCCCCAACACCGAGTTGTGAAGGTGA AGGGCTGCACCCtCCAGGAGGACCCCCCGACAGAGTGGCAAGTACATCAAGAGCTTGTGGAGAGA GTGCTGAAGAACGAGCAGgatccgc GGCCATCATCAAGGAGTTCATCGCCTTAAGGTGCACATGGAGGGCTCCGTGAACGGCCACGAGTTCGAGA TCGAGGGCGAGGGCGAGGGCGCCCCTACGAGGGCACCCAGACCGCCAAGCTGAAGGTGACCAAGGGTGGC CCCCGGCCCTTCGCTGGGACATCTGTCCCCCTCAGTTCATGTACGGCTCAAGGCCACGTGAAGCACC CGCCGACATCCCCGACTACTTGAAGCTGTCCTTCCCCGAGGGCTTCAAGTGGAGCGCGTGTGAACTTCG AGGACGGCGCGTGGTGACCGTAGCCAGGACTCTCCCTGCAGGACGGGAGTTCATCTACAAGGTGAAG CTGCGCGGCCACCAACTTCCCCCTCGACGGGCCGCTGAAGGGCGAGATCAAGCAGAGGCTGAAGCTGAAGGACGGCG GCCACTACGACGCTGAGGTCAAGACCACCTACAAGGCCAAGAAGGCCGACGTGCCCCGCGCTACAAC GTCAACATCAAGTTGGACATCACCTCCACAACGAGGACTACACCATCGTGAACAGTACGAACGCCGA GGGCCGCACTCCACCGGGCATGGACGAGCTGTACAAGAagcttcgcgcgcactcgagcaccaccacc accaccactga

SUPPLEMENTAL NOTES

***EcYcgR* mutations.** The R113L mutation (M1) in YNL-EcYcgR was predicted to change the c-di-GMP binding stoichiometry from 2:1 to 1:1 as well as reduce affinity for c-di-GMP based on analysis of the corresponding mutant in the YcgR protein PP4397 from *P. putida*.⁵ As expected, M1 showed reduced affinity in the lysate-based assay (Figure S2b). Measurements with purified protein confirmed the reduced affinity and showed that binding stoichiometry was very slightly reduced compared to WT (Figure S2c). The oligomeric states of c-di-GMP are dependent on the ions present, with potassium (present at 100 mM in the binding assay buffer) promoting the formation of higher order oligomeric complexes, which may have complicated measurements of the binding stoichiometry.^{5,6}

The R118D mutation (M2) in YNL-EcYcgR was predicted to knock out binding for c-di-GMP, as this residue should make key interactions with the phosphate linkage of c-di-GMP. This mutation effectively ablated binding to c-di-GMP, as expected.

The S147A mutation (M3) in the YNL-EcYcgR scaffold was predicted to modestly improve affinity for c-di-GMP based on literature measurements (Ryjenkov *et al.* reported a K_D change from $0.84 \pm 0.16 \mu\text{M}$ to $0.69 \mu\text{M}$ for full-length EcYcgR⁷), but our lysate-based measurements showed slightly reduced affinity instead. This discrepancy may be due to differences in the protein constructs, the assay methods (Ryjenkov *et al.* used equilibrium dialysis with purified protein), and buffer conditions. Interestingly, the corresponding mutant in PP4397 has a 4-fold reduced affinity as measured by ITC, which is in line with our result.⁵

Due to additive effects, the S147A/R113L double mutation (M4) showed poorer affinity than either M1 or M3 mutation alone.

M1, M3, and M4 mutations to YNL-EcYcgR unexpectedly led to decreased signal changes (Figure S2c). These mutations to the c-di-GMP binding pocket may subtly alter the conformation of the bound or unbound state of the sensor domain.

Linker screen. The different linker regions tested in YNL-EcYcgR all showed decreased signal changes compared to the original linker sequence used (Figure S2d). While no crystal structure is available for EcYcgR that would allow for a rational design of the linker regions, crystal structures of the homologous YcgR protein PP4397 from *P. putida* provide some degree of insight into the relative distance and orientation of the N- and C-termini in YcgR proteins. PP4397 was analyzed in the phylogenetic screen (sequence 2 in Figure S4a) and was found to behave very

similarly to EcYcgR, which suggests that their overall structures are likely similar. In the apo x-ray crystal structure of full length PP4397 (PDB ID: 2GJG), the distance between C α atoms of the N- and C-termini is ~25.7 Å. This distance appears to be too long to be bridged by the original linker that gave a functional YNL-EcYcgR biosensor, which was 2 residues. However, we note that the first ~11 N-terminal residues and the last ~3 C-terminal residues are largely unstructured, so may serve as flexible linkers on their own.

Prior to this structural analysis, we had designed new linkers to be either flexible or rigid with varying lengths from 2 to 5 residues. All of the linkers tested showed similarly decreased signal changes compared to the original linker, which suggests that they led to increased interaction of RLuc halves in the unbound state. These results indicate that shortening the linkers or truncating the YcgR protein may lead to improved signal change and/or brightness for YNL-EcYcgR, but these changes are unlikely to be directly translatable to other phylogenetic variants, which are of different lengths. Since the original linkers were applied successfully to YNL-EcYcgR and other Nano-lantern-based biosensors,⁸ they were carried forward to the phylogenetic screen.

Supplemental References

- (1) Gibson, D. G., Young, L., Chuang, R. Y., Venter, J. C., Hutchison, C. A., and Smith, H. O. (2009) Enzymatic assembly of DNA molecules up to several hundred kilobases. *Nat. Methods* 6, 343–345.
- (2) Oberortner, E., Cheng, J. F., Hillson, N. J., and Deutsch, S. (2017) Streamlining the Design-to-Build Transition with Build-Optimization Software Tools. *ACS Synth. Biol.* 6, 485–496.
- (3) McKenna, A., Hanna, M., Banks, E., Sivachenko, A., Cibulskis, K., Kernytsky, A., Garimella, K., Altshuler, D., Gabriel, S., Daly, M., and DePristo, M. A. (2010) The Genome Analysis Toolkit: A MapReduce framework for analyzing next-generation DNA sequencing data. *Genome Res.* 20, 1297–1303.
- (4) Studier, F. W. (2005) Protein production by auto-induction in high-density shaking cultures. *Protein Expr. Purif.* 41, 207–234.
- (5) Ko, J., Ryu, K. S., Kim, H., Shin, J. S., Lee, J. O., Cheong, C., and Choi, B. S. (2010) Structure of PP4397 reveals the molecular basis for different c-di-GMP binding modes by pilZ domain proteins. *J. Mol. Biol.* 398, 97–110.
- (6) Zhang, Z., Kim, S., Gaffney, B. L., and Jones, R. A. (2006) Polymorphism of the signaling molecule c-di-GMP. *J. Am. Chem. Soc.* 128, 7015–7024.
- (7) Ryjenkov, D. A., Simm, R., Römling, U., and Gomelsky, M. (2006) The PilZ domain is a receptor for the second messenger c-di-GMP: The PilZ domain protein YcgR controls motility in enterobacteria. *J. Biol. Chem.* 281, 30310–30314.
- (8) Saito, K., Chang, Y.-F., Horikawa, K., Hatsugai, N., Higuchi, Y., Hashida, M., Yoshida, Y., Matsuda, T., Arai, Y., and Nagai, T. (2012) Luminescent proteins for high-speed single-cell and whole-body imaging. *Nat. Commun.* 3, 1262.